Current Biology, Vol. 15, 1006–1015, June 7, 2005, ©2005 Elsevier Ltd All rights reserved. DOI 10.1016/j.cub.2005.04.061

Wsh3/Tea4 Is a Novel Cell-End Factor Essential for Bipolar Distribution of Tea1 and Protects Cell Polarity under Environmental Stress in *S. pombe*

Hisashi Tatebe,[1] Koichi Shimada,[1,3] Satoru Uzawa,[2] Susumu Morigasaki,[1] and Kazuhiro Shiozaki[1,*]
[1]Section of Microbiology
Division of Biological Sciences
University of California, Davis
Davis, California 95616
[2]Department of Biochemistry and Biophysics
University of California, San Francisco
San Francisco, California 94143

Summary

Background: The fission yeast *Schizosaccharomyces pombe* has a cylindrical cell shape, for which growth is strictly limited to both ends, and serves as an excellent model system for genetic analysis of cell-polarity determination. Previous studies identified a cell-end marker protein, Tea1, that is transported by cytoplasmic microtubules to cell tips and recruits other cell-end factors, including the Dyrk-family Pom1 kinase. The Δ*tea1* mutant cells cannot grow in a bipolar fashion and show T-shaped morphology after heat shock.
Results: We identified Wsh3/Tea4 as a novel protein that interacts with Win1 MAP kinase kinase kinase (MAPKKK) of the stress-activated MAP kinase cascade. Wsh3 forms a complex with Tea1 and is transported to cell tips by growing microtubules. The Δ*wsh3* mutant shows monopolar growth with abnormal Tea1 aggregate at the non-growing cell end; this abnormal aggregate fails to recruit Pom1 kinase. Consistent with the observed interaction between Win1 and Wsh3, cells lacking Wsh3 or Tea1 show more severe cell-polarity defects under osmolarity and heat-stress stimuli that are known to activate the stress MAPK cascade. Furthermore, mutants of the stress MAPK also exhibit cell-polarity defects when exposed to the same stress.
Conclusions: Wsh3/Tea4 is an essential component of the Tea1 cell-end complex. In addition to its role in bipolar growth during the normal cell cycle, the Wsh3-Tea1 complex, together with the stress-signaling MAPK cascade, contributes to cell-polarity maintenance under stress conditions.

Introduction

A eukaryotic intracellular signaling module, the mitogen-activated protein kinase (MAPK) cascade, transmits signals through sequential activation of three tiers of protein kinases, MAP kinase kinase kinase (MAPKKK), MAPK kinase, and MAPK [1]. In a number of signal-transduction pathways from yeast to humans, MAPK cascades link cell surface receptors to nuclear transcription factors and regulate gene expression in response to extracellular stimuli [2–4]. Although less well characterized, MAPKs also control cytoplasmic processes. For example, phosphorylation of the myosin light-chain kinase (MLCK) by MAPK in the cytoplasm is believed to regulate cell motility [5]. Another striking example for non-nuclear functions of MAPK is that the JIP (JNK Interacting Protein) scaffold proteins, which tether the stress-activated MAPK cascades, are transported away from the nucleus by kinesin, a plus-end-directed microtubule motor protein [6, 7]. In developing neurons, JIP proteins transported along the microtubules accumulate at the tips of extending neurites [8–10]. Studies of JIP-deficient animals suggest that JIP proteins play roles in axonal vesicle transport and morphogenesis of the nervous systems [11, 12].

The fission yeast *Schizosaccharomyces pombe* has a cylindrical cell shape, which is maintained through exclusive tip growth [13]. This highly polarized cell morphology is established by cytoplasmic microtubules that emanate from microtubule-organizing centers (MTOCs) on the nuclear envelope and extend toward both cell tips [14–16]. Plus ends of growing microtubules carry the cell-end marker protein, Tea1; once they reach cell tips, Tea1 is deposited to the cell cortex, establishing the specific bipolar localization of Tea1 [17]. The cell-end localization of Tea1 is also dependent on the Tea2 kinesin [18], a microtubule plus-end-tracking protein called Tip1 [19], as well as the Mod5 protein, which is anchored to the cell-tip plasma membrane through its C-terminal lipid modification [20]. Gel filtration and density-gradient centrifugation experiments suggest that Tea1 forms multiple high-molecular-weight protein complexes with other proteins that also function at cell tips [17, 21]. Loss of the Tea1 protein complexes in the Δ*tea1* mutant results in mislocalization of other cell-end factors, such as Tea3 [22], Bud6/Aip3 [23, 24], and a Dyrk-family protein kinase, Pom1 [25].

Although absence of Tea1 does not lead to the loss of the cylindrical cell morphology, the Δ*tea1* mutant is often bent and grows only in a monopolar fashion, in contrast to bipolar growth of wild-type cells [17]. It was also reported that the cell-polarity defect of Δ*tea1* is exacerbated after a heat shock that shifts the culture temperature from 25°C to 36°C, leading to T-shaped morphology [17]. These observations imply that Tea1 may play a role under certain stress conditions, in addition to its function during the normal cell cycle.

Here, we report a novel *S. pombe* cell-end protein, Wsh3/Tea4, which moves to cell tips by forming a complex with Tea1 and is essential for formation of the functional Tea1 complex at cell tips. Strikingly, we isolated Wsh3 in a yeast two-hybrid screen for its interaction with Win1 MAPKKK of the stress-activated Spc1 MAPK cascade. Spc1 [26], also known as Sty1 [27], is a structural, functional ortholog of the mammalian stress MAPKs, such as p38 and JNK, and is responsive to diverse forms of environmental stress, including high osmolarity and heat shock [28, 29]. Indeed, the cell-branching phenotypes in the Δ*wsh3* and Δ*tea1* mutants are significantly accentuated after heat shock and high osmolarity, stress stimuli that activate the Spc1 MAPK

*Correspondence: kshiozaki@ucdavis.edu
[3]Present address: Department of Periodontology, Nihon University School of Dentistry, Chiyoda-ku, Tokyo 101-8310, Japan.

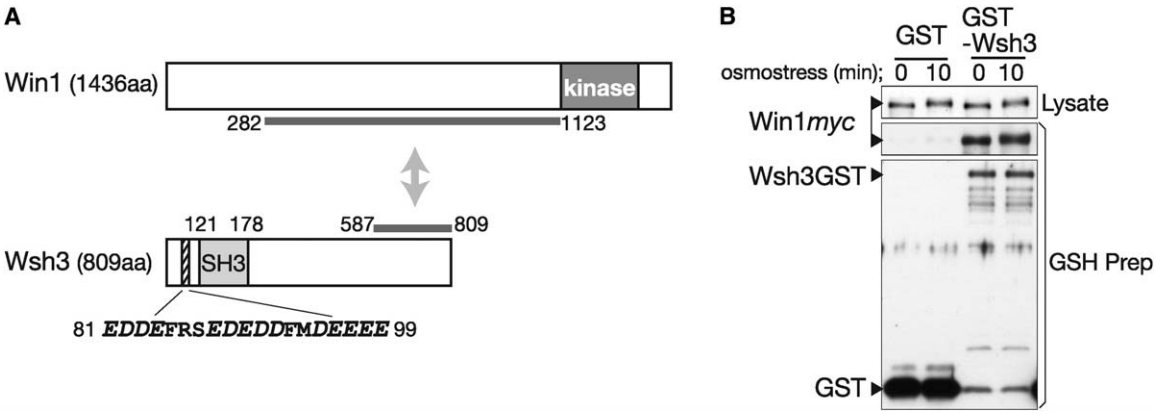

Figure 1. Wsh3 Interacts with Win1 MAPKKK

(A) The sequence encoding residues 282–1123 within the noncatalytic extension of Win1 was used as bait in the yeast two-hybrid screen. cDNA clones encoding the C-terminal region of Wsh3 (residues 587–809) were repeatedly isolated in the screen for an interaction with the Win1 bait.

(B) Win1 is coprecipitated with Wsh3. *win1:myc* Δ*wsh3* strains carrying a plasmid expressing either GST or GST-Wsh3 were harvested before and 10 min after high-osmolarity stress induced by 0.6 M KCl. Proteins purified by glutathione-Sepharose beads (GSH Prep) were analyzed via immunoblots with anti-*myc* and anti-GST antibodies. Win1 shows a gel-mobility shift upon activation by osmostress.

cascade. We propose that, in addition to its role in bipolar cell growth, the Tea1-Wsh3 complex contributes to the maintenance of cell polarity under stress conditions that affect the cytoskeleton.

Results

Isolation of Wsh3 as a Novel MAPKKK-interacting Protein

Aiming to discover proteins that regulate the activity and/or function of the stress-responsive Spc1 MAPK cascade, we searched for proteins interacting with the non-catalytic domain of Win1 MAPKKK [30] by yeast two-hybrid screens. These screens repeatedly isolated cDNA clones containing an open reading frame SPBC1706.01; we named this gene *wsh3*$^+$ (Win1-interacting SH3-domain protein). Wsh3 is a 809-amino acid, 89.5 kDa protein with a Src homology 3 (SH3) domain at residues 121–178, as well as a cluster of acidic amino acid residues at positions 81–99 (Figure 1A). A database search indicated that Wsh3 shares a weak sequence similarity with the budding yeast Bud14, which is involved in bipolar bud site selection [31, 32]. Other published fungal genome sequences also contain potential orthologs (data not shown).

Interaction between Win1 MAPKKK and Wsh3 was also detected biochemically in *S. pombe*. Wsh3 was overexpressed from a plasmid with an N-terminal GST (glutathione *S*-transferase) tag, and isolation of GST-Wsh3 by glutathione-Sepharose led to coprecipitation of Win1 both before and after high osmolarity stress that activates the Spc1 MAPK cascade (Figure 1B). However, despite repeated attempts, we failed to detect significant copurification of the endogenous Wsh3 and Win1 proteins (data not shown); their physical association may not be strong enough to survive protein dilution during cell-lysate preparation.

The *wsh3* Mutant Shows Cell-Polarity Defects Accentuated by Stress Conditions

To examine the cellular function of Wsh3, we constructed the *wsh3* null (Δ*wsh3*) strain by the gene-disruption technique. We found that the haploid Δ*wsh3* mutant was viable and had a doubling time similar to that of *wsh3*$^+$ strains (data not shown). We quantified Spc1 MAPK activation under different stress conditions by immunoblotting with the antibodies that specifically crossreact with the phosphorylated, active Spc1 [33]. Spc1 activation in Δ*wsh3* cells was comparable to that in wild-type cells, suggesting that Wsh3 does not affect the stress activation of Win1 MAPKKK for signaling to Spc1 MAPK (data not shown).

However, under stress conditions, Δ*wsh3* cells showed significant morphological defects. After shifting to high-osmolarity medium containing 0.6 M KCl or 1 M sorbitol, 20%–30% of Δ*wsh3* cells exhibited highly bent or branched morphology (Figure 2A). Heat-shock treatment that shifted cultures from 25°C to 36°C also had similar effects on the Δ*wsh3* morphology. On the other hand, oxidative stress by hydrogen peroxide, which also induces Spc1 activation [34], did not significantly affect Δ*wsh3* cells (data not shown). These observations indicate that Wsh3 function is important to maintain growth polarity under high osmolarity stress and heat shock, and the loss of Wsh3 leads to initiation of an abnormal growth site.

The aberrant cell morphology of the Δ*wsh3* mutant resembles the reported cell-polarity defects of *tea* mutants, which were isolated for their T-shaped morphology [35, 36]. The branching phenotype of the *tea* mutants is dramatically enhanced in the *cdc11* cytokinesis mutant, which repeats nuclear division cycles without cytokinesis [36]. We also found that the Δ*wsh3* mutation induced cell branching at a high frequency in the *cdc11* background after shifting up to its restrictive temperature (Figure 2B). In early G2, *S. pombe* cells

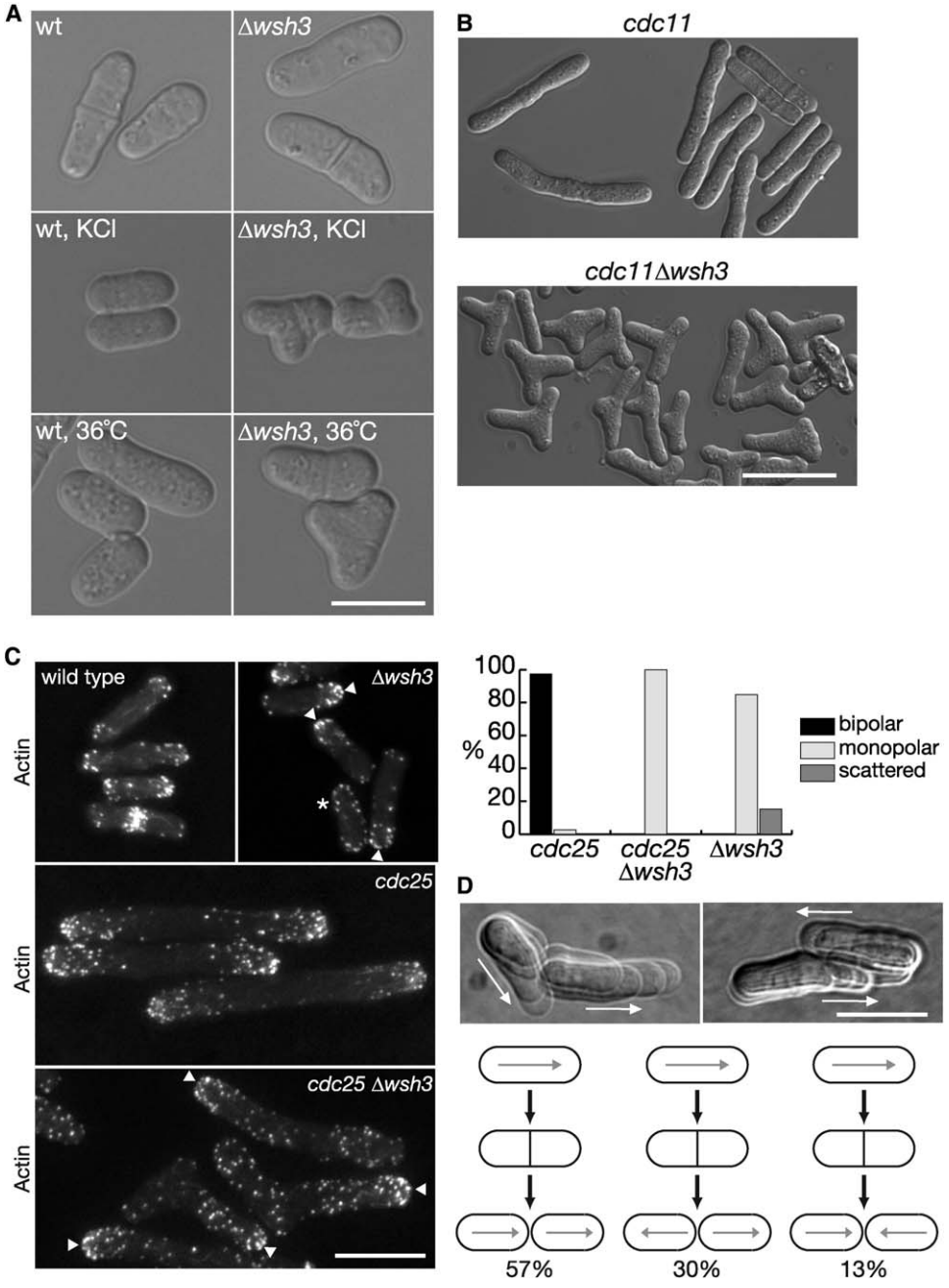

Figure 2. Δ*wsh3* Shows Defects in Cell Polarity

(A) Wild-type and Δ*wsh3* strains grown in YES medium were photographed before and after stress induced by either 0.6 M KCl for 3 hr or a temperature shift from 25°C to 36°C for 3 hr. The scale bar represents 10 μm.

(B) The cell-polarity defect of Δ*wsh3* is accentuated in the *cdc11* background. *cdc11-132* and *cdc11-132* Δ*wsh3* strains were grown in YES medium at 25°C, followed by incubation at 36°C for 4 hr. The scale bar represents 20 μm.

(C) Monopolar distribution of actin by the Δ*wsh3* mutation (arrowheads). Wild-type and Δ*wsh3* strains were grown at 30°C. *cdc25-22* and *cdc25-22* Δ*wsh3* strains were grown at 25°C, followed by incubation at 36°C for 3.5 hr. Actin was stained with rhodamine-phalloidin. In some Δ*wsh3* cells, actin patches are scattered and not polarized (indicated by an asterisk). The scale bar represents 10 μm. Frequencies of the actin distribution patterns are shown as a graph on the right.

(D) The Δ*wsh3* mutant shows monopolar growth. Δ*wsh3* cells were grown on YES agar medium and imaged by time-lapse microscopy. (Top) Two pairs of daughter cells are shown. Arrows and outlines of cells at later time points indicate the growth direction of cells. The scale bar represents 10 μm. (Bottom) Summary of growth end selection patterns in Δ*wsh3*. Twenty-six samples were examined.

switch from monopolar to bipolar growth, a process known as NETO (new end take off) [37]. However, like *tea1* mutants [36], Δ*wsh3* cells were found to grow exclusively in a monopolar fashion. Actin patches, which are localized to the growing tips of fission-yeast cells [38], were detected mostly in one tip of the Δ*wsh3* cell (Figure 2C). This observation was further confirmed with the *cdc25*-22 mutant that arrests in late G2 and continues bipolar growth with actin patches at both cell tips (Figure 2C, middle panel). On the other hand, the *cdc25*-22 Δ*wsh3* cells exhibited monopolar growth, and actin patches were mostly concentrated to one cell tip, although some actin patches showed depolarized localization (bottom panel). Time-lapse observation of growing Δ*wsh3* cells (Figure 2D) demonstrated that dividing daughter cells initiated cell growth at either old or new ends and continued monopolar growth.

Wsh3 Forms a Complex with the Cell-End Marker Protein Tea1

Because of the observed role of Wsh3 in growth polarity, we examined the cellular localization of Wsh3 by tagging the chromosomal *wsh3*$^+$ gene with the green fluorescent protein (GFP) sequence (Figure 3A). The majority of Wsh3-GFP was concentrated at both cell tips and could also be observed as dots in the cytoplasm. In dividing cells, the Wsh3-GFP signal was also detected as a medial band (Figure 3A, right panel). These specific localization patterns of Wsh3 appeared to be dependent on cellular microtubules; the cell-end localization of Wsh3-GFP was abrogated by a β-tubulin mutation, *nda3-KM311* [39], even at its permissive temperature, 30°C (Figure 3B, left). Consistently, treatment with microtubule inhibitors thiabendazole (TBZ) and methyl benzimidazol-2yl carbamate (MBC) significantly reduced accumulation of Wsh3-GFP at cell tips (data not shown).

The localization pattern of Wsh3 and its microtubule dependency are very similar to those of the cell-end marker protein Tea1, which is localized at plus ends of growing microtubules and is deposited at cell tips [17, 20, 40]. Indeed, by using a strain that coexpresses the GFP-fused α tubulin and Wsh3 fused to the red fluorescent protein (RFP) [41], we observed that Wsh3-RFP localized at the tip of growing microtubules was transported toward cell ends (Figure 3B, right). To further characterize the behavior of Wsh3-GFP in living cells, we employed a microscope system (named OMX) recently developed by John W. Sedat and David A. Agard (Experimental Procedures). In the OMX system, as one 3D-data-acquisition modality, during each exposure the sample stage of the microscope is moved in a linear fashion along the z axis as a focus sweep through the thickness of samples (typically 3–5 μm for fission-yeast cells), so that all signals throughout the cell are projected as one two-dimensional image. Each 2D image was deconvolved by computation [42]. OMX allows rapid data acquisition at close time points (50 ms exposure at one projection/s throughout this study). Using this system, we captured the Wsh3-GFP localization in living *S. pombe* cells every second over 10 min (Movie S1, in the Supplemental Data available with this article online). To trace the movement of individual Wsh3-GFP dots over time, we converted the movie to the stereo kymograph image shown in Figure 3C. Most Wsh3 dots appeared around the middle of the cell and moved toward cell tips at an average of approximately 3 μm/min, a speed similar to that of the Tea1 dot movement [40].

Furthermore, we found that the normal Wsh3 distribution is dependent on Tea1. The specific localization of Wsh3-GFP was lost in the Δ*tea1* mutant, and the Wsh3-GFP signal was diffused throughout the cytoplasm (Figure 4A). These results suggest that Wsh3 is localized at cell tips and cytoplasmic dots through its binding to Tea1. Consistent with this model, association between the Wsh3 and Tea1 proteins in cell lysates was detected by coprecipitation experiments (Figure 4B). Furthermore, significant overlaps of cellular localization of Wsh3 and Tea1 were confirmed with a *tea1:GFP* strain in which the chromosomal *wsh3*$^+$ gene was tagged with the RFP sequence (Figure 4C).

Taken together, these results strongly suggest that Wsh3 forms a complex with Tea1 and is transported to cell tips by the cytoplasmic microtubule system in a Tea1-dependent manner.

Wsh3 Is Essential for Bipolar Localization of the Cell-End Marker Tea1 and the Pom1 Protein Kinase

To further characterize the role of Wsh3 in cell-polarity determination, we tested whether Wsh3 affects the localization of Tea1 (Figure 5A). In *wsh3*$^+$ cells, Tea1-GFP was clearly observed at both cell tips, as reported previously [17]. In contrast, most Δ*wsh3* cells showed highly concentrated Tea1-GFP signals at one end, whereas the other end contained significantly less Tea1-GFP dots (Figure 5A, right panel). Because the Δ*wsh3* mutant grows in a monopolar fashion (Figure 2), we examined whether this biased Tea1 localization correlates with the tip-growth pattern of Δ*wsh3* cells; concentrated actin patches and the Tea1-GFP accumulation were localized at opposite ends of Δ*wsh3* cells (Figure 5B). Thus, the Tea1-accumulating tip of Δ*wsh3* cells is not capable of growth.

Live-cell imaging of Tea1-GFP with the OMX system (Figure 5C) showed that, in wild-type cells (Movie S2), Tea1 dots appeared around the middle of the cell and moved toward both cell tips (Figure 5C, left panels), as previously reported [17, 40]. The kymograph that is expanded for the tip region (Figure 5C [i]) shows that the Tea1-GFP pattern altered with time, suggesting the dynamic nature of the cell-end structure containing Tea1. This was in clear contrast with the kymograph of the Tea1-accumulating cell tip of the Δ*wsh3* strain (Figure 5C [v]); except for gradual photobleaching, very little change was observed during the experiment. Transport of Tea1-GFP dots to the opposite end of the Δ*wsh3* cell was also observed (Figure 5C [iv] and Movie S3), but these dots often disappeared after they reached the cell tip and never accumulated to the levels observed in wild-type cells (Figure 5C [iii]).

Pom1 is a member of the Dyrk-family protein kinase and localized at cell tips in a Tea1-dependent manner [25]. In the Δ*wsh3* cells, the cell-end localization of Pom1 was lost, and Pom1-GFP often accumulated in vesicle-like structures in the cytoplasm (Figure 5D). Immunoblotting analysis indicated that the Pom1 protein

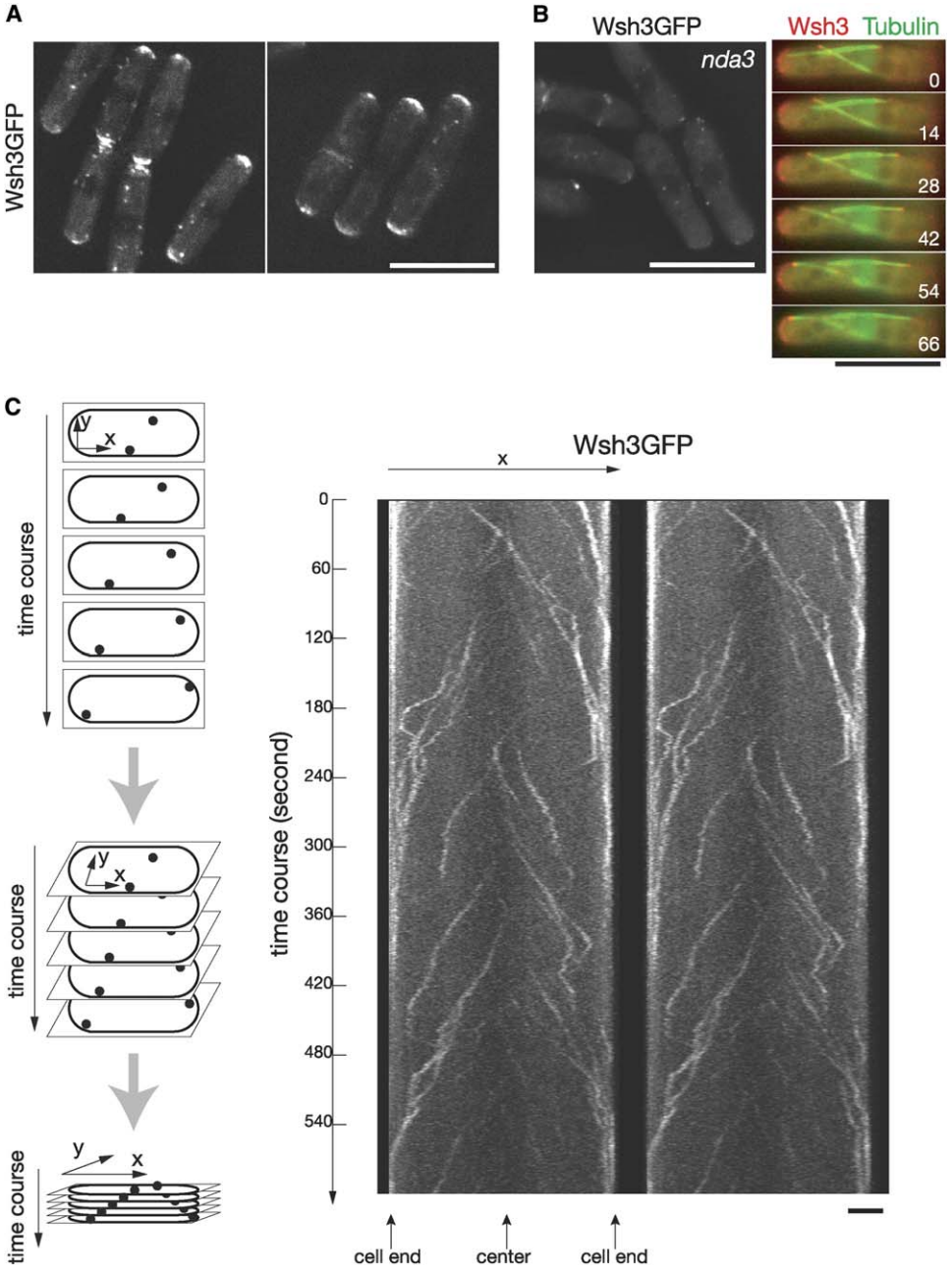

Figure 3. Cellular Localization of Wsh3

(A) A wild-type strain whose chromosomal *wsh3*$^{+}$ gene is fused with the sequence encoding GFP (*wsh3:GFP*) was observed by deconvolution microscopy. The scale bar represents 10 μm.

(B) Microtubule-dependent Wsh3 transport. (Left) A *nda3-KM311* strain carrying the *wsh3:GFP* allele was grown at 30°C and observed by deconvolution microscopy. (Right) Time-lapse microscopy of a *wsh3:RFP* strain expressing GFP-α tubulin. Numbers indicate the times in seconds. Scale bars represent 10 μm.

(C) Cytoplasmic Wsh3 speckles move toward cell tips. Sequential images of a single *wsh3:GFP* cell were taken at 1 s intervals for 10 min at room temperature and converted to a stereo kymograph that displays Wsh3 speckle movements through the time course in both x and y (perpendicular to the images) axes (see the schematic representation on the left). The dark region in the middle corresponds to the position of the nucleus. The scale bar represents 2 μm.

level was not significantly altered between wild-type and Δ*wsh3* strains (data not shown). These results suggest that the Tea1-containing structures at cell tips of Δ*wsh3* are not functional and cannot recruit Pom1 kinase. Consistently, the Δ*wsh3* defects described above (Figure 2) are very similar to the phenotypes of Pom1-defective strains [25, 43]; both Δ*wsh3* and Δ*pom1* mutants showed monopolar growth, and their branching

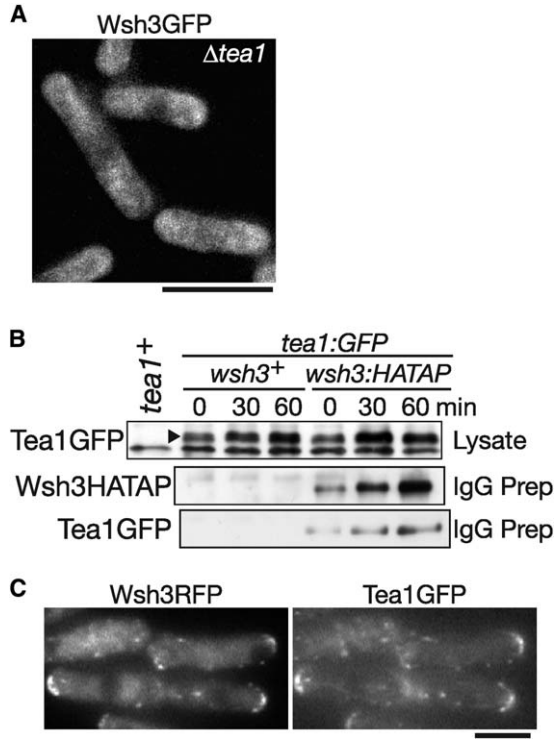

Figure 4. Wsh3 Interacts with Tea1 In Vivo

(A) Wsh3 is delocalized in the Δ*tea1* mutant. A Δ*tea1 wsh3:GFP* strain grown at 30°C was observed by deconvolution microscopy. The scale bar represents 10 μm.

(B) Tea1 forms a complex with Wsh3. *tea1:GFP* and *tea1:GFP wsh3:HATAP* strains grown at 30°C were treated with high-osmolarity stress conditions of 0.6 M KCl and harvested at the indicated time points. Wsh3HATAP was purified by IgG-Sepharose, followed by immunoblotting with anti-GFP and anti-HA antibodies. An arrowhead indicates the position of Tea1GFP as detected by anti-GFP antibodies.

(C) Wsh3 is colocalized with Tea1. A *wsh3:RFP tea1:GFP* strain was grown at 30°C in EMM liquid medium, and a single focal plane was captured for RFP and GFP signals. The scale bar represents 5 μm.

morphology was enhanced in the *cdc11* background. We also observed branched-cell morphology with the Δ*pom1* strain after osmostress and heat shock (data not shown). In addition, their division septum was often misplaced from the center of the cell (Figure 5E). These observations strongly suggest that the Pom1 kinase is not functional in the Δ*wsh3* mutant. Consistently, the Δ*wsh3* Δ*pom1* double mutant exhibited stress-induced morphological defects similar to those of the Δ*wsh3* single mutant (data not shown). On the other hand, cellular localization of Wsh3-GFP appeared to be normal in Δ*pom1* cells, indicating that the Pom1 function is not required for the proper localization of Wsh3 (data not shown).

Wsh3, Tea1, and Spc1 MAPK Contribute to Cell-Polarity Maintenance under Stress Conditions

As described above, Wsh3 interacts with Win1 MAPKKK of the stress MAPK cascade, and the Δ*wsh3* mutant shows cell-polarity defects, which are accentuated by stress stimuli that activate the MAPK cascade. Because Wsh3 forms a complex with Tea1, we examined whether the Tea1 function might also be important under these stress conditions. It was previously reported that Δ*tea1* cells exhibit branching at high frequency after the temperature shift from 25°C to 36°C (Figure 6A; [17, 20, 44]). We found that high-osmolarity stress by 0.6 M KCl also promotes the appearance of T-shaped cells in the Δ*tea1* strain, to levels comparable to those of the Δ*wsh3* mutant (Figure 6B). The Δ*wsh3* Δ*tea1* double and Δ*wsh3* Δ*tea1* Δ*pom1* triple mutants exhibited T-shaped morphology at slightly higher frequencies than the Δ*tea1* and Δ*wsh3* single mutants under stress conditions. These results suggest that the Tea1-Wsh3 complex plays a role in maintaining growth polarity under osmostress and heat shock.

To assess the involvement of the Spc1 MAPK cascade in cell-polarity maintenance under stress, we examined the morphology of Δ*spc1* cells under various stress conditions. Spc1 is essential for cellular survival of stress through transcriptional induction of resistance genes, and the Δ*spc1* mutant ceases cell growth and loses viability under stress conditions [26, 27, 45]. Because expression of cell-polarity phenotypes requires cell growth, we chose mild stress conditions that allowed cell growth of the Δ*spc1* mutant. Cell-polarity defects with bent and branched morphology were observed after the Δ*spc1* mutant was shifted from 25°C to 36°C (Figure 6C). We also found that, even under optimal growth conditions, the Δ*spc1* mutation exacerbates the morphology defects of the Δ*tea1* mutant; Δ*tea1* Δ*spc1* double mutants grown at 30°C in rich YES medium contain large fractions of significantly bent and branched cells (Figure 6D).

These observations suggest that, together with Wsh3-Tea1 complex, the Spc1 MAPK cascade contributes to cell-polarity maintenance, particularly under osmostress and heat-shock conditions.

Discussion

In this paper, we have identified a novel SH3-domain protein, Wsh3, which forms a complex with the Tea1 cell-end marker protein and is required for proper Tea1 distribution and function; a new gene name, *tea4*$^{+}$, was recently reserved for *wsh3*$^{+}$ in the *S. pombe* GeneDB (http://www.genedb.org/genedb/pombe/index.jsp). Wsh3/Tea4 was isolated through its interaction with the stress MAPKKK, Win1. Indeed, both Δ*wsh3* and Δ*tea1* mutants exhibit cell branching under high-osmolarity and heat-shock conditions, indicating that the Wsh3/Tea4-Tea1 complex is required for maintaining cell polarity under environmental stress.

Both cytological and biochemical data strongly suggest that Wsh3/Tea4 binds to Tea1 and that the complex is transported to cell tips by growing microtubules. On the other hand, in the Δ*wsh3* mutant, cytoplasmic dots of the Tea1-GFP are transported toward cell tips but fail to accumulate at one cell end; they instead form an abnormal static aggregate at the other end. Therefore, Wsh3/Tea4 is not required for the localization of Tea1 to microtubule plus ends but plays an essential role in building functional Tea1-containing structures in

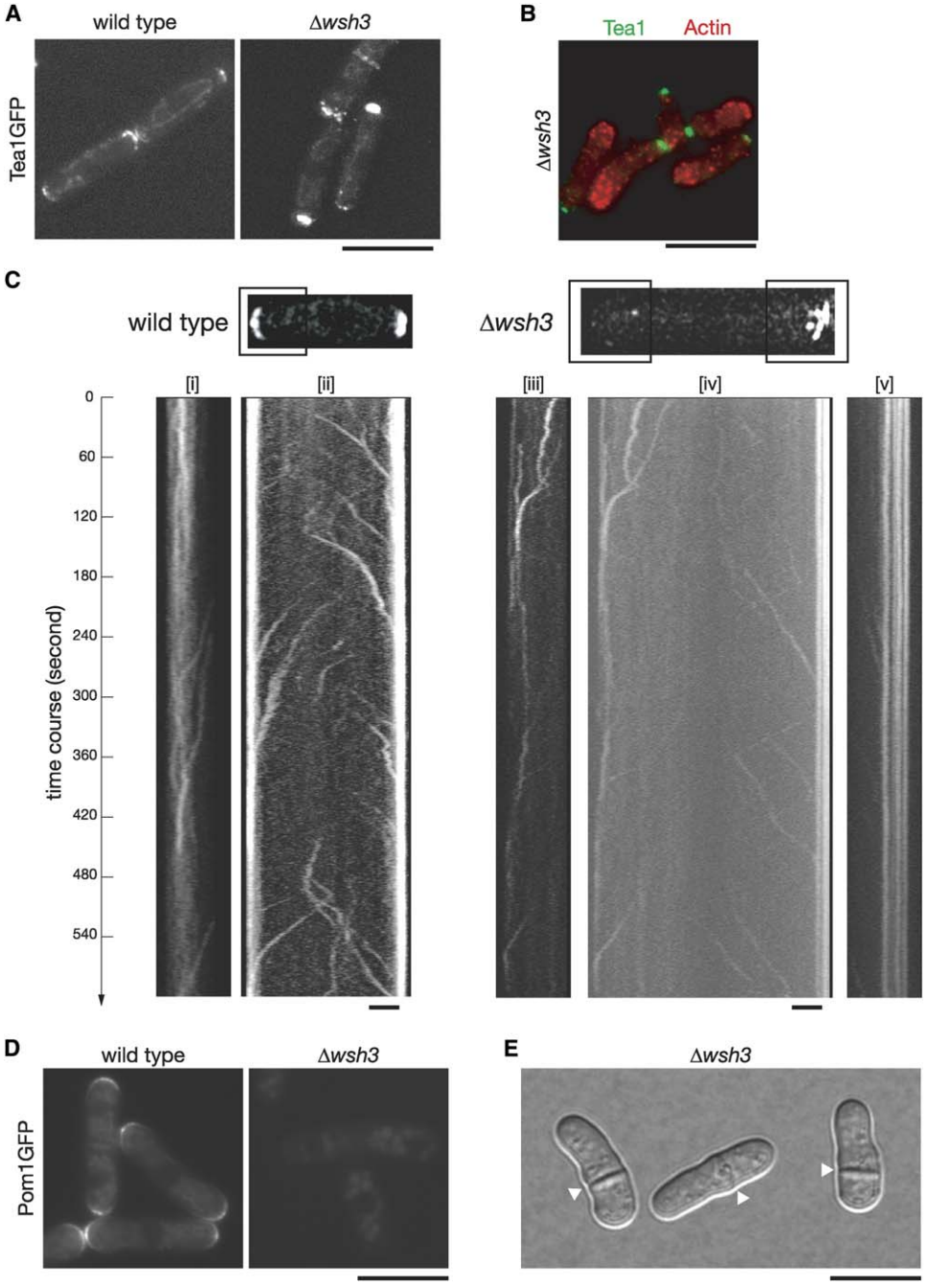

Figure 5. Wsh3 Is Required for Normal Tea1 Localization

(A) Tea1 is concentrated at one end of the Δ*wsh3* cell. Wild-type and Δ*wsh3* strains carrying the *tea1:GFP* allele were grown at 30°C and observed by deconvolution microscopy. The scale bar represents 10 μm.

(B) Actin is concentrated at the Tea1-free cell tip. A Δ*wsh3 tea1:GFP* strain was stained for Tea1GFP and actin by anti-GFP antibodies and rhodamine-phalloidin, respectively. The scale bar represents 10 μm.

(C) The behavior of Tea1GFP at cell tips in wild-type and Δ*wsh3* cells. Sequential images of a single *tea1:GFP* cell and a single *tea1:GFP* Δ*wsh3* cell were taken at 1 s intervals for 10 min at room temperature and converted to kymographs, which represent Tea1 dot movements in the cytoplasm. In panels (i), (iii), and (v), kymographs at cell-tip regions (shown by squares on cell images above) are further spread out to show the Tea1 movements in these areas. The scale bar represents 2 μm.

(D) Pom1 is delocalized in Δ*wsh3*. Wild-type and Δ*wsh3* strains carrying the *pom1:GFP* allele were grown at 30°C and observed by fluorescence microscopy. The scale bar represents 10 μm.

(E) Septum displacement in Δ*wsh3* cells. A Δ*wsh3* strain grown in YES medium was pictured by DIC microscopy. Arrowheads indicate positions of division septa.

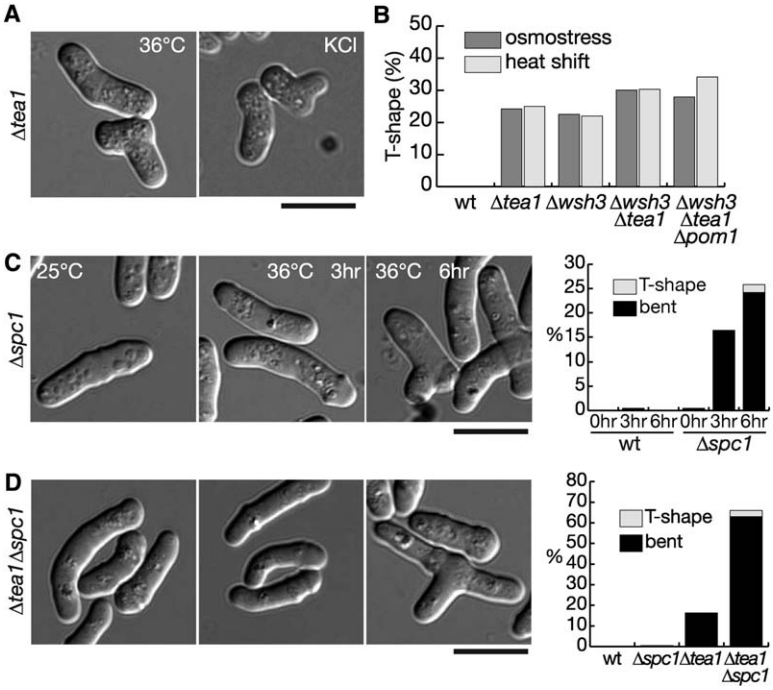

Figure 6. Environmental Stress Exacerbates the Cell-Polarity Defects of Δ*tea1*, Δ*wsh3*, and Δ*spc1* Mutants

(A) A Δ*tea1* strain was grown in YES medium at 25°C. Cells were observed 3 hr after stress of either a temperature shift from 25°C to 36°C or 0.6 M KCl. The scale bar represents 10 μm.

(B) Appearance of T-shaped cells in wild-type, Δ*tea1*, Δ*wsh3*, Δ*wsh3* Δ*tea1*, and Δ*wsh3* Δ*tea1* Δ*pom1* strains was monitored 3 hr after osmostress induced by 0.6 M KCl and a temperature shift from 25°C to 36°C. At least 200 cells were examined in each sample.

(C) Cell-polarity defects in Δ*spc1* upon heat shock. A wild-type strain and a Δ*spc1* strain were grown in YES medium at 25°C and observed for T-shaped or severely bent cells at the indicated time points after the temperature shift to 36°C. At least 150 cells were examined in each sample. The scale bar represents 10 μm.

(D) Synthetic morphological defects in the Δ*tea1* Δ*spc1* double mutant. Wild-type, Δ*spc1*, Δ*tea1*, and Δ*tea1* Δ*spc1* strains were grown at 30°C in YES medium. More than 120 cells were examined in each sample. The scale bar represents 10 μm.

a bipolar fashion. Consistently, Pom1 kinase, which is anchored to cell tips in a Tea1-dependent manner [25], cannot localize properly in the Δ*wsh3* mutant. This Dyrk-family protein kinase is a major determinant of the tip-directed cell growth, and the Δ*pom1* mutant is defective in bipolar growth and septum positioning [25, 46]. These phenotypes are similar to those of Δ*wsh3*, indicating that mislocalization of Pom1 in Δ*wsh3* cells results in the loss of Pom1 function. Together, data presented in this paper establish that Wsh3/Tea4 is a novel cell-polarity factor essential for the bipolar localization and function of the cell-end marker, Tea1.

Although Wsh3-Win1 interaction was reproducibly detected by both yeast two-hybrid and GST-Wsh3 pull-down experiments, concentrated localization of Win1 or Wis4 MAPKKKs to cell tips is not detectable (our unpublished results). Therefore, the Wsh3/Tea4-Win1 interaction may be transient, or Wsh3/Tea4 may recruit only a small subpopulation of the MAPKKK to the Tea1 complex. The following observations further corroborate a link between the Wsh3/Tea4-Tea1 complex and the Spc1 MAPK cascade. A temperature shift from 25°C to 36°C significantly increases the frequency of cell branching in both Δ*tea1* and Δ*pom1* mutants [17, 25]. We found that not only heat shock but also high-osmolarity stress accentuates the cell-polarity defects in the Δ*tea1* and Δ*pom1* mutants, as in the Δ*wsh3* mutants. These mutants also exhibit severe polarity defects when they exit the stationary phase and resume cell growth [20] (data not shown). Importantly, all of these conditions, heat shock, high osmolarity, and recovery from the stationary phase, induce activation of the Spc1 MAPK cascade [26, 27, 34] (our unpublished results). Moreover, the Δ*spc1* mutant itself shows bent and branched cell morphologies under mild stress conditions. In addition, the Pyp1 tyrosine phosphatase, which dephosphorylates and inactivates Spc1 MAPK [26, 27], suppresses *orb4* and *orb12*, cell-polarity mutants that exhibit a round cell shape [36]. Together with the detected Wsh3–Win1 MAPKKK interaction, these results suggest that the Tea1-Wsh3/Tea4 complex and the stress MAPK cascade play important roles in cell-polarity maintenance under stressful conditions. It is conceivable that the Wsh3/Tea4-recruited Spc1 cascade modulates the Tea1 complex through phosphorylation because Δ*wis1* and a mutant expressing a catalytically inactive Spc1 MAPK show cell-morphology defects similar to those of Δ*spc1* cells (our unpublished results). Exact molecular function of Spc1-dependent phosphorylation in cell polarity has not been determined; the Δ*spc1* mutation affects neither the Wsh3/Tea4-Tea1 association nor their cell-end accumulation either before or after stress (our unpublished results). Identification of the direct Spc1 substrate in this context will be necessary if we are to understand the exact role of the MAPK in cell polarity.

Previous studies indicated that Tea1, Pom1, and other cell-end factors are required for the establishment of growth sites during the normal cell cycle; mutants lacking these proteins are unable to initiate a second growth site for bipolar growth [13, 47]. Why do the Tea1-Wsh3/Tea4 complex and the stress MAPK cascade become important under stress conditions? One likely possibility is that environmental stress has significant impacts on the cytoskeleton and that, therefore, cells require active adaptation mechanisms to protect or reorganize the polarized cytoskeletal structures. It is known that high-osmolarity stress induces disassembly of the actin cytoskeleton [48, 49]. We also observed that, after osmostress, the dynamic polymerization/depolymerization cycle of microtubules is almost completely stalled, a dramatic change detectable only by

time-lapse observation of living cells (Supplemental Data). Dynamic instability is a built-in characteristic of microtubules, which undergo continuous polymerization and depolymerization, and the static microtubule structures in osmostressed cells are quite unexpected. Although the mechanism for this transient loss of microtubule dynamics is currently unknown, such a dramatic change is likely to affect the cell-polarity machinery in light of the central role of the microtubule system in the establishment of growth sites in *S. pombe*.

A recent study of mutant mice lacking JNK1 suggests that the mammalian stress MAPK is involved in microtubule dynamics of neuronal cells, in addition to its role in regulation of the c-Jun transcription factor in the nucleus [50]. The involvement of the stress-responsive MAPK in linking extracellular environment to cellular cytoskeleton may be evolutionarily conserved, with some variations specific to organisms. Because of its genetic tools and ease of microtubule studies, fission yeast is expected to serve as an excellent model for studying the interaction of the stress MAPK cascade with the cytoskeletal systems.

Experimental Procedures

Yeast Strains and General Techniques

S. pombe strains used in this study are listed in Table S1. Detailed procedures for strain construction are described in the Supplemental Data. Growth media and basic techniques for *S. pombe* have been described [51]. *S. pombe* cells were grown in yeast extract medium YES and synthetic medium EMM. Stress treatments of *S. pombe* cultures have been described previously [33]. TBZ (Sigma) and MBC (Sigma) were used at final concentrations of 100 μg/ml and 25 μg/ml, respectively.

Yeast Two-Hybrid Screen

The *win1*$^+$ sequence has a pair of repetitive sequences, which prevents amplification in *E. coli* [30]. Therefore, we introduced two silent mutations at 1278 (T→G) and 1281 (A→G) in *win1*$^+$ and cloned the fragment encoding amino acid residues 282–1123 into pGBT8 for expression as a fusion with the Gal4 DNA binding domain (pGBT8-Win1N). Using an *S. pombe* cDNA library in pGADGH and a budding-yeast strain HF7c [52], we screened approximately 1.0 × 10^8 transformants by histidine prototrophy and β-galactosidase assay. A HF7c strain carrying pGBT8-Win1N and the pGADGH vector as well as that carrying the pGBT8 vector and pGADGH-Wsh3 were histidine auxotrophic, confirming the specificity of the Win1–Wsh3 interaction in the two-hybrid assay.

Protein Coprecipitation Experiments

For GST pull-down experiments, cells carrying the pREP1KZ-Wsh3 (GST-Wsh3) plasmid were grown in EMM liquid medium lacking thiamine at 30°C for 12 hr to induce expression of GST-Wsh3 proteins. Cells were suspended in GST lysis buffer (50 mM Tris-HCl [pH 8.0], 5 mM EDTA, 400 mM NaCl, 10% glycerol, 0.1 mM Na_3VO_4, 1 mM β-mercaptoethanol, 0.5% Triton X-100) containing protease inhibitors and lysed by vortexing with glass beads, and centrifugation followed. The soluble crude lysate was incubated with glutathione Sepharose 4B (Amersham Biosciences) at 4°C for 30 min. Immunoblotting was performed with mouse monoclonal anti-*myc* antibodies (9E10, BAbCO) and rabbit polyclonal anti-GST antibodies.

For affinity purification of the TAP-tagged Wsh3, cells grown in YES medium were harvested and suspended in IP buffer (50 mM Tris-HCl [pH7.2], 5 mM EDTA, 150 mM NaCl, 10% glycerol, 50 mM NaF, 0.1 mM Na_3VO_4, 1 mM β-mercaptoethanol, and 0.5% Triton X-100) containing protease inhibitors. Cells were lysed by vortexing with glass beads, and centrifugation followed. The soluble crude lysate was incubated with IgG Sepharose 6 (Amersham Biosciences) at 4°C for 2 hr. Immunoblotting was performed with mouse monoclonal anti-HA antibodies (12CA5, Boehringer Mannheim) and rabbit polyclonal anti-GFP antibodies (sc-8334, Santa Cruz Biotechnology).

Microscopy

Experimental procedures for the OMX optical microscope can be found in the Supplemental Data. This new microscope system will also be described in the near future in a publication. For other microscopy, an Eclipse E600 microscope (Nikon), equipped with a 60× oil-immersion objective lens and a digital charge-coupled-device camera (Orca C4742-95, Hamamatsu) was used for data acquisition (see Supplemental Data). Openlab (Improvision) and Adobe Photoshop (Adobe Systems) were used for capturing images and figure preparation, respectively.

Supplemental Data

Supplemental Data are available with this article online at http://www.current-biology.com/cgi/content/full/15/11/1006/DC1/.

Acknowledgments

We are grateful to J. Sedat for allowing us to use the OMX system, R. Maximo, G. Lam, J. Rust, and P. Novy for technical assistance, K. Nakano for advice, and J. Sedat and A. Ikner for critical reading of the manuscript. P. Nurse, M. Yanagida, T. Toda, T. Matsumoto, D. Hirata, K. Sawin, N. Rhind, and R. Tsien kindly provided strains and plasmids. H.T. was a recipient of the JSPS (Japan Society for the Promotion of Science) Postdoctoral Fellowship for Research Abroad and the Uehara Memorial Foundation Postdoctoral Fellowship. This research was supported by a National Institutes of Health grant (GM59788) awarded to K.S.

Received: March 10, 2005
Revised: April 22, 2005
Accepted: April 25, 2005
Published online: May 5, 2005

References

1. Widmann, C., Gibson, S., Jarpe, M.B., and Johnson, G.L. (1999). Mitogen-activated protein kinase: Conservation of a three-kinase module from yeast to human. Physiol. Rev. *79*, 143–180.
2. Treisman, R. (1996). Regulation of transcription by MAP kinase cascades. Curr. Opin. Cell Biol. *8*, 205–215.
3. Gustin, M.C., Albertyn, J., Alexander, M., and Davenport, K. (1998). MAP kinase pathways in the yeast *Saccharomyces cerevisiae*. Microbiol. Mol. Biol. Rev. *62*, 1264–1300.
4. Yang, S.H., Sharrocks, A.D., and Whitmarsh, A.J. (2003). Transcriptional regulation by the MAP kinase signaling cascades. Gene *320*, 3–21.
5. Klemke, R.L., Cai, S., Giannini, A.L., Gallagher, P.J., de Lanerolle, P., and Cheresh, D.A. (1997). Regulation of cell motility by mitogen-activated protein kinase. J. Cell Biol. *137*, 481–492.
6. Goldstein, L.S. (2001). Kinesin molecular motors: Transport pathways, receptors, and human disease. Proc. Natl. Acad. Sci. USA *98*, 6999–7003.
7. Morrison, D.K., and Davis, R.J. (2003). Regulation of MAP kinase signaling modules by scaffold proteins in mammals. Annu. Rev. Cell Dev. Biol. *19*, 91–118.
8. Meyer, D., Liu, A., and Margolis, B. (1999). Interaction of c-Jun amino-terminal kinase interacting protein-1 with p190 rhoGEF and its localization in differentiated neurons. J. Biol. Chem. *274*, 35113–35118.
9. Yasuda, J., Whitmarsh, A.J., Cavanagh, J., Sharma, M., and Davis, R.J. (1999). The JIP group of mitogen-activated protein kinase scaffold proteins. Mol. Cell. Biol. *19*, 7245–7254.
10. Verhey, K.J., Meyer, D., Deehan, R., Blenis, J., Schnapp, B.J., Rapoport, T.A., and Margolis, B. (2001). Cargo of kinesin identified as JIP scaffolding proteins and associated signaling molecules. J. Cell Biol. *152*, 959–970.
11. Byrd, D.T., Kawasaki, M., Walcoff, M., Hisamoto, N., Matsu-

moto, K., and Jin, Y. (2001). UNC-16, a JNK-signaling scaffold protein, regulates vesicle transport in *C. elegans*. Neuron *32*, 787–800.

12. Kelkar, N., Delmotte, M.H., Weston, C.R., Barrett, T., Sheppard, B.J., Flavell, R.A., and Davis, R.J. (2003). Morphogenesis of the telencephalic commissure requires scaffold protein JNK-interacting protein 3 (JIP3). Proc. Natl. Acad. Sci. USA *100*, 9843–9848.
13. Hayles, J., and Nurse, P. (2001). A journey into space. Nat. Rev. Mol. Cell Biol. *2*, 647–656.
14. Hagan, I.M., and Hyams, J.S. (1988). The use of cell division cycle mutants to investigate the control of microtubule distribuition in the fission yeast *Schizosaccharomyces pombe*. J. Cell Sci. *89*, 343–357.
15. Drummond, D.R., and Cross, R.A. (2000). Dynamics of interphase microtubules in *Schizosaccharomyces pombe*. Curr. Biol. *10*, 766–775.
16. Sagolla, M.J., Uzawa, S., and Cande, W.Z. (2003). Individual microtubule dynamics contribute to the function of mitotic and cytoplasmic arrays in fission yeast. J. Cell Sci. *116*, 4891–4903.
17. Mata, J., and Nurse, P. (1997). tea1 and the microtubular cytoskeleton are important for generating global spatial order within the fission yeast cell. Cell *89*, 939–949.
18. Browning, H., Hayles, J., Mata, J., Aveline, L., Nurse, P., and McIntosh, J.R. (2000). Tea2p is a kinesin-like protein required to generate polarized growth in fission yeast. J. Cell Biol. *151*, 15–28.
19. Brunner, D., and Nurse, P. (2000). CLIP170-like tip1p spatially organizes microtubular dynamics in fission yeast. Cell *102*, 695–704.
20. Snaith, H.A., and Sawin, K.E. (2003). Fission yeast mod5p regulates polarized growth through anchoring of tea1p at cell tips. Nature *423*, 647–651.
21. Feierbach, B., Verde, F., and Chang, F. (2004). Regulation of a formin complex by the microtubule plus end protein tea1p. J. Cell Biol. *165*, 697–707.
22. Arellano, M., Niccoli, T., and Nurse, P. (2002). Tea3p is a cell end marker activating polarized growth in *Schizosaccharomyces pombe*. Curr. Biol. *12*, 751–756.
23. Glynn, J.M., Lustig, R.J., Berlin, A., and Chang, F. (2001). Role of bud6p and tea1p in the interaction between actin and microtubules for the establishment of cell polarity in fission yeast. Curr. Biol. *11*, 836–845.
24. Jin, H., and Amberg, D.C. (2001). Fission yeast Aip3p (spAip3p) is required for an alternative actin-directed polarity program. Mol. Biol. Cell *12*, 1275–1291.
25. Bähler, J., and Pringle, J.R. (1998). Pom1p, a fission yeast protein kinase that provides positional information for both polarized growth and cytokinesis. Genes Dev. *12*, 1356–1370.
26. Shiozaki, K., and Russell, P. (1995). Cell-cycle control linked to the extracellular environment by MAP kinase pathway in fission yeast. Nature *378*, 739–743.
27. Millar, J.B.A., Buck, V., and Wilkinson, M.G. (1995). Pyp1 and Pyp2 PTPases dephosphorylate an osmosensing MAP kinase controlling cell size at division in fission yeast. Genes Dev. *9*, 2117–2130.
28. Nguyen, A.N., and Shiozaki, K. (2002). MAPping stress survival in yeasts: From the cell surface to the nucleus. In Sensing, Signaling and Cell Adaptation, Volume 3, K.B. Storey and J.M. Storey, eds. (Amsterdam: Elsevier Science), pp. 75–90.
29. Toone, W.M., and Jones, N. (2004). Stress responses in *S. pombe*. In The Molecular Biology of *Schizosaccharomyces pombe*, R. Egel, ed. (Heidelberg: Springer-Verlag), pp. 57–72.
30. Samejima, I., Mackie, S., Warbrick, E., Weisman, R., and Fantes, P.A. (1998). The fission yeast mitotic regulator *win1*$^{+}$ encodes a MAP kinase kinase kinase that phosphorylates and activates Wis1 MAP kinase kinase in response to high osmolarity. Mol. Biol. Cell *9*, 2325–2335.
31. Ni, L., and Snyder, M. (2001). A genomic study of the bipolar bud site selection pattern in *Saccharomyces cerevisiae*. Mol. Biol. Cell *12*, 2147–2170.
32. Cullen, P.J., and Sprague, G.F., Jr. (2002). The Glc7p-interacting protein Bud14p attenuates polarized growth, pheromone response, and filamentous growth in *Saccharomyces cerevisiae*. Eukaryot. Cell *1*, 884–894.
33. Shiozaki, K., and Russell, P. (1997). Stress-activated protein kinase pathway in cell cycle control of fission yeast. Methods Enzymol. *283*, 506–520.
34. Degols, G., Shiozaki, K., and Russell, P. (1996). Activation and regulation of the Spc1 stress-activated protein kinase in *Schizosaccharomyces pombe*. Mol. Cell. Biol. *16*, 2870–2877.
35. Snell, V., and Nurse, P. (1993). Investigations into the control of cell form and polarity: the use of morphological mutants in fission yeast. Dev. Suppl. *1993*, 289–299.
36. Verde, F., Mata, J., and Nurse, P. (1995). Fission yeast cell morphogenesis: Identification of new genes and analysis of their role during the cell cycle. J. Cell Biol. *131*, 1529–1538.
37. Mitchison, J.M., and Nurse, P. (1985). Growth in cell length in the fission yeast *Schizosaccharomyces pombe*. J. Cell Sci. *75*, 357–376.
38. Marks, J., Hagan, I.M., and Hyams, J.S. (1986). Growth polarity and cytokinesis in fission yeast: The role of the cytoskeleton. J. Cell Sci. Suppl. *5*, 229–241.
39. Umesono, K., Toda, T., Hayashi, S., and Yanagida, M. (1983). Cell division cycle genes *nda2* and *nda3* of the fission yeast *Schizosaccharomyces pombe* control microtubular organization and sensitivity to anti-mitotic benzimidazole compounds. J. Mol. Biol. *168*, 271–284.
40. Behrens, R., and Nurse, P. (2002). Roles of fission yeast tea1p in the localization of polarity factors and in organizing the microtubular cytoskeleton. J. Cell Biol. *157*, 783–793.
41. Campbell, R.E., Tour, O., Palmer, A.E., Steinbach, P.A., Baird, G.S., Zacharias, D.A., and Tsien, R.Y. (2002). A monomeric red fluorescent protein. Proc. Natl. Acad. Sci. USA *99*, 7877–7882.
42. Agard, D.A., Hiraoka, Y., Shaw, P., and Sedat, J.W. (1989). Fluorescence microscopy in three dimensions. Methods Cell Biol. *30*, 353–377.
43. Bähler, J., and Nurse, P. (2001). Fission yeast Pom1p kinase activity is cell cycle regulated and essential for cellular symmetry during growth and division. EMBO J. *20*, 1064–1073.
44. Sawin, K.E., and Nurse, P. (1998). Regulation of cell polarity by microtubules in fission yeast. J. Cell Biol. *142*, 457–471.
45. Chen, D., Toone, W.M., Mata, J., Lyne, R., Burns, G., Kivinen, K., Brazma, A., Jones, N., and Bähler, J. (2003). Global transcriptional responses of fission yeast to environmental stress. Mol. Biol. Cell *14*, 214–229.
46. Niccoli, T., Arellano, M., and Nurse, P. (2003). Role of Tea1p, Tea3p and Pom1p in the determination of cell ends in *Schizosaccharomyces pombe*. Yeast *20*, 1349–1358.
47. Chang, F. (2001). Establishment of a cellular axis in fission yeast. Trends Genet. *17*, 273–278.
48. Chowdhury, S., Smith, K.W., and Gustin, M.C. (1992). Osmotic stress and the yeast cytoskeleton: Phenotype-specific suppression of an actin mutation. J. Cell Biol. *118*, 561–571.
49. Rupes, I., Jia, Z., and Young, P.G. (1999). Ssp1 promotes actin depolymerization and is involved in stress response and new end take-off control in fission yeast. Mol. Biol. Cell *10*, 1495–1510.
50. Chang, L., Jones, Y., Ellisman, M.H., Goldstein, L.S., and Karin, M. (2003). JNK1 is required for maintenance of neuronal microtubules and controls phosphorylation of microtubule-associated proteins. Dev. Cell *4*, 521–533.
51. Alfa, C., Fantes, P., Hyams, J., McLeod, M., and Warbrick, E. (1993). Experiments with Fission Yeast. A laboratory course manual (Cold Spring Harbor, NY: Cold Spring Harbor Press).
52. Feilotter, H.E., Hannon, G.J., Ruddell, C.J., and Beach, D. (1994). Construction of an improved host strain for two hybrid screening. Nucleic Acids Res. *22*, 1502–1503.

Note Added in Proof

Wsh3/Tea4 was also recently reported as a cell-polarity factor that interacts with both Tea1 and the formin For3 (Martin, S.G., McDonald, W.H., Yates, J.R. and Chang, F. (2005) Dev. Cell *8*, 479-491).